Tandem electrocatalytic N_2 fixation via concerted proton-electron transfer

Pablo Garrido-Barros, Joseph Derosa, Matthew J. Chalkley, Jonas C. Peters*

Division of Chemistry and Chemical Engineering, California Institute of Technology; Pasadena, CA 91125, USA.

*Corresponding author. Email: jpeters@caltech.edu

ABSTRACT: New electrochemical ammonia (NH_3) synthesis technologies are of interest as a complementary route to the Haber-Bosch (HB) process for distributed fertilizer generation, and towards exploiting ammonia as a zero-carbon fuel produced via renewably-sourced electricity. Apropos of these goals is a surge of fundamental research targeting heterogeneous materials as electrocatalysts for the nitrogen reduction reaction (N_2RR). These systems generally suffer from poor stability and NH_3 selectivity; competitive hydrogen evolution reaction (HER) outcompetes N_2RR. Molecular catalyst systems can be exquisitely tuned and offer an alternative strategy, but progress has thus far been thwarted by the same selectivity issue; HER dominates. Herein we describe a tandem catalysis strategy that offers a solution to this puzzle. A molecular complex that can mediate an N_2 reduction cycle is partnered with a co-catalyst that interfaces the electrode and an acid to mediate concerted proton-electron transfer (CPET) steps, facilitating N–H bond formation at a favorable applied potential and overall thermodynamic efficiency. Without CPET, certain intermediates of the N_2RR cycle would be unreactive via independent electron transfer (ET) or proton transfer (PT) steps, thereby shunting the system. Promisingly, complexes featuring several metals (W, Mo, Os, Fe) achieve N_2RR electrocatalysis at the same applied potential in the presence of the CPET mediator, pointing to the generality of this tandem approach.

In the drive to develop electrocatalytic strategies for ammonia synthesis that complement HB (Figure 1a),[1–8] molecular catalysts offer a number of distinct advantages. In particular, they can be carefully tuned to satisfy the electronic requirements of N_2 binding and activation. They can also afford access to insightful mechanistic studies at the level of critical bond-breaking and making steps. Remarkable progress has been made over the past two decades in terms of chemically driven N_2RR catalysis and mechanistic understanding using molecular systems.[9–12] Despite this, bona fide N_2RR electrocatalysis in this domain remains virtually unknown;[13–16] only one such synthetic electrocatalyst (a tris(phosphine)borane iron ((TPB)Fe) system from our lab, Figure 1b) has been reliably demonstrated, but it requires low temperatures (−35 °C) to mitigate background HER, operates with low turnover, and requires a highly reducing potential (−2.1 V vs ferrocenium/ferrocene, $Fc^{+/0}$; all potentials herein are reported vs $Fc^{+/0}$).[17] This state of affairs sharply contrasts the substantial progress that has been made applying molecular systems towards electrocatalytic HER, the carbon dioxide reduction reaction (CO_2RR), and the oxygen reduction reaction (ORR), among other transformations.[18–21]

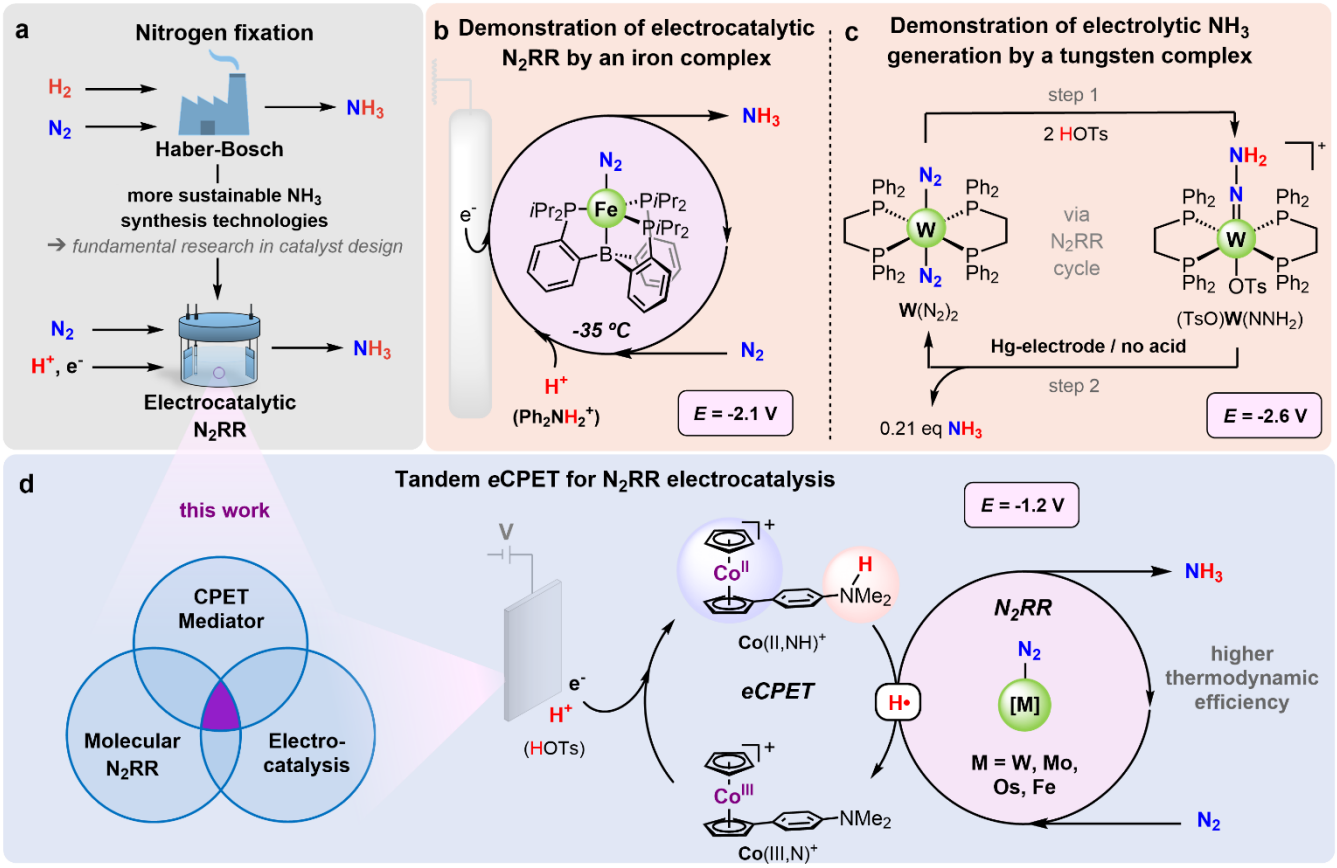

Figure 1. (a) Nitrogen fixation based on the traditional Haber-Bosch (HB) process versus electrochemical approaches to N_2RR that require fundamental research in catalyst design. (b) The only molecular N_2RR electrocatalyst reported thus far based on the (TPB)Fe system operating at −2.1 V on a glassy carbon electrode using at temperature of −35 °C. (c) Early work by Pickett demonstrating electro-generation of NH_3 using the molecular complex **W**$(N_2)_2$ at an applied potential of −2.6 V on a Hg-pool electrode using tosic acid (TsOH). The acidolysis step 2 had to be performed separately from the reduction step (0.21 equiv NH_3 / **W**$(N_2)_2$ after one cycle; 0.73 equiv total NH_3 / **W**$(N_2)_2$ after three cycles). (d) Tandem catalysis described in this work based on coupling the CPET mediator, **Co**(II,NH)$^+$, with molecular N_2RR catalysts to enable well-defined electrocatalysis at comparatively mild potentials (−1.2 V using TsOH).

Akin to candidate heterogeneous electrocatalysts, molecular systems typically mediate HER in preference to N_2RR, and/or operate at such reducing potentials that background HER at a working electrode dominates. Pioneering research from 1985 by Pickett and coworkers underscored this point (Figure 1c). In a study involving a bis(diphenylphosphinoethane)tungsten (abbreviated throughout as **W**) system, they showed that the hydrazido complex (TsO)**W**$(NNH_2)^+$ (TsO = tosylate), generated via protonation of the bis-N_2 adduct **W**$(N_2)_2$ by tosic acid (TsOH), releases NH_3 (0.21 equiv NH_3 per **W**) upon application of a highly reducing potential (−2.6 V on a Hg-pool electrode), but only in the absence of the acid.[22] In follow-up work, attempts to render this tungsten system electrocatalytic using various electrodes in the presence of acids led to even lower NH_3 yields (≤ 0.1 equiv NH_3 per **W**).[23] Strategies that attenuate the HER rate, for example by positively shifting the operating potential while still maintaining a significant N_2RR rate, are essential. Scaling relationships have historically frustrated such an approach; as the operating potential for reductive electrocatalysis is tuned

positively, the rate of the desired transformation decreases.[24,25] Therefore, pathways to break such scaling relationships to achieve efficient electrocatalytic N_2RR at comparatively mild potentials are needed.

Recent work from our lab introduced a strategy for attenuating the rate of (electro)catalytic HER. Via the use of a concerted proton-electron transfer (CPET) mediator, comprised of cobaltocenium modified by a tethered Brønsted base (abbreviated herein as **Co**(III,N)$^+$; Figure 1d),[26] catalyzed HER is prevented. This mediator design spatially and electronically separates the proton and electron relays, key to storing highly reactive H atom equivalents as **Co**(II,NH)$^+$ at a potential that is sufficiently mild to also mitigate background HER at the electrode. Initial model studies using this mediator established that electrochemical CPET (*e*CPET) provides a means to reduce unsaturated organic substrates by applying a comparatively mild potential in the presence of tosic acid.[26,27]

While these results point to the possibility of applying such a mediator towards electrocatalytic N_2RR, the mediator itself does not react with N_2, in contrast to unsaturated organic substrates. Hence, we have pursued a tandem catalysis strategy (Figure 1d) pairing a candidate molecular catalyst that can bind N_2 (M–N_2) and facilitate its multistep reduction to NH_3 through various M–N_xH_y intermediates (e.g., M–N=NH, M=NNH_2, M=NH),[9] with a CPET mediator that interfaces the electrode and the acid with the N_2 reduction cycle via critical CPET steps. Importantly, certain N_2RR intermediates are challenging to move through the cycle; they can be difficult to independently reduce or protonate (vide infra). In principle, a CPET step can circumvent this issue and favorably shift the overpotential needed to drive the net electrochemical N_2RR process. Here we show the feasibility of this tandem catalysis strategy, demonstrating N_2RR electrocatalysis in solution at room temperature and atmospheric N_2 pressure at a comparatively mild potential (−1.2 V) in the presence of tosic acid.

As a model system to test our tandem approach, we adapted the classical tungsten system studied by Pickett.[22] Using **W**$(N_2)_2$ and the same solvent (tetrahydrofuran; THF), electrolyte (0.2 M [TBA][BF_4]; TBA = tetra-*N*-butylammonium), and acid (100 equiv TsOH), in the presence of the cobalt CPET mediator, **Co**(III,N)$^+$, a controlled potential electrolysis (CPE) produced 4.7 ± 0.3 equiv NH_3 at 18 ± 2% Faradaic efficiency (FE) over a period of 11 hours using a glassy carbon (GC) electrode at −1.35 V (see Supplementary Information, section S3). Reloading the system with an additional 100 equiv TsOH furnished a total of 7.6 equiv NH_3. While further improvements in yield and turnover are discussed next, this initial result shows that inclusion of the **Co**(III,N)$^+$ mediator turns on electrocatalysis by **W**$(N_2)_2$, and at a potential that is 1.25 V positive of Pickett's original work (Figure 1c). In the absence of the mediator, electrocatalysis is not observed.

To further improve electrocatalytic N_2RR by this tandem **W**$(N_2)_2$/**Co**(III,N)$^+$ co-catalyst system, we canvassed factors including the working electrode, the loading of TsOH, the electrolyte, and the solvent (see Supplementary Information, section S4). We found that boron-doped diamond (BDD) as a working electrode, known to better mitigate background HER than GC,[28] enhanced NH_3 selectivity. Using lithium triflimide ([Li][NTf_2]), which features a hard Lewis acid and a robust, non-coordinating anion, proved favorable to [TBA][BF_4] as the electrolyte. Also, we found dimethoxyethane (DME) to be a more robust ethereal solvent than THF for this electrocatalysis. Optimized conditions (BDD, 0.1 M [Li][NTf_2], DME, 5 mM TsOH, 0.05 mM **W**$(N_2)_2$/**Co**(III,N)$^+$) significantly improved the N_2RR electrocatalysis with 11.5 equiv NH_3 per **W**$(N_2)_2$/**Co** (45% FE) being generated at −1.35 V over 5.5 hours (Figure 2a,b).

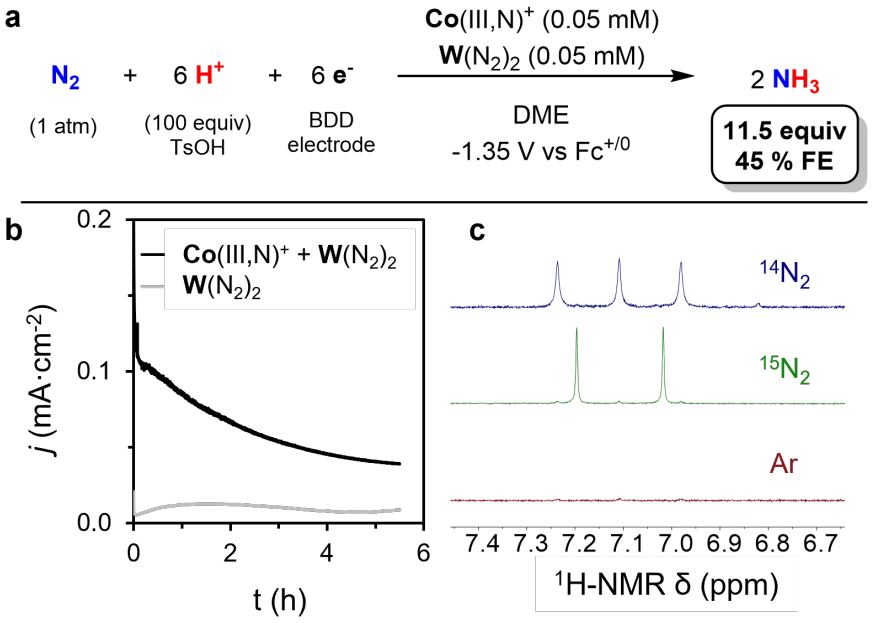

Figure 2. (a) Electrocatalytic N_2RR upon controlled potential electrolysis (CPE) at −1.35 V vs $Fc^{+/0}$ in 0.1 M [Li][NTf_2] DME solution containing 0.05 mM **Co**(III,N)$^+$, 0.05 mM **W**$(N_2)_2$, and 5 mM TsOH, using a BDD plate working electrode. (b) Current profile for the CPE experiment described (black trace) and a similar CPE experiment in the absence of the **Co**(III,N)$^+$ mediator. (c) Quantification of NH_3 following CPE via ^{1}H-NMR spectroscopy under previous conditions using either $^{14}N_2$, $^{15}N_2$, or an argon atmosphere.

When **Co**(III,N)$^+$ was omitted, only 0.8 equiv NH_3 per **W**$(N_2)_2$ were obtained under these same conditions. Excluding **W**$(N_2)_2$ instead afforded < 0.1 equiv NH_3 per **Co**(III,N)$^+$ (Table S1). Control experiments to assess the purity of the N_2 gas, studying the electrocatalysis under argon instead of N_2 (< 0.1 equiv NH_3 per **W**$(N_2)_2$/**Co**(III,N)$^+$), or under $^{15}N_2$ (8.1 equiv $^{15}NH_3$ per **W**$(N_2)_2$/**Co**(III,N)$^+$), unequivocally demonstrate N_2 as the sole N-source of the NH_3 produced (see Figure 2c and section S5 of the Supplementary Information). Finally, rinsing the electrodes following a CPE and performing an analogous experiment with fresh acid but in the absence of **W**$(N_2)_2$/**Co**(III,N)$^+$ resulted in no NH_3 production (< 1 nmol). A higher turnover number per **W**$(N_2)_2$/**Co**(III,N)$^+$ (up to 39.5) was demonstrated by using a higher surface area GC foam electrode and lowering the catalyst concentration (Table S1).

To assess the electrochemical behavior of the **W**$(N_2)_2$/**Co**(III,N)$^+$ co-catalyst system, a series of cyclic voltammograms (CVs) were performed. Following prior studies, dissolution of **W**$(N_2)_2$ in THF with added TsOH acid quantitatively produces the doubly protonated hydrazido complex (TsO)**W**$(NNH_2)^+$.[23] CVs of (TsO)**W**$(NNH_2)^+$ in a 0.1 M [Li][NTf_2] THF solution on a BDD working electrode show two irreversible one-electron waves at low potential (< −2 V, Figure 3a). In accord with prior literature, these are presumed due to the generation of **W**$(NNH_2)^+$ and **W**(NNH_2), respectively,[22] where the strongly reducing potential reflects the challenge in reducing the 18-electron, closed-shell (TsO)**W**$(NNH_2)^+$ complex. While the addition of excess TsOH (100 equiv) to the solution containing (TsO)**W**$(NNH_2)^+$ led to an increase in current (irreversible) with an onset at −1.3 V, the same response is observed without added **W** and is due to background HER at the electrode (Figure 3a). The independent CV of **Co**(III,N)$^+$ in THF shows a reversible $Co^{III/II}$ couple at −1.35 V (Figure 3b), assigned to **Co**(III,N)$^+$/**Co**(II,N).[26] This couple shifts to −1.21 V when the mediator is protonated at the tethered dimethylaniline group (i.e., **Co**(III,NH)$^{2+}$/**Co**(II,NH)$^+$) (Figure 3a). Gratifyingly, CVs of (TsO)**W**$(NNH_2)^+$ in the presence of **Co**(III,N)$^+$ result in a fully irreversible, multi-electron wave at −1.2 V (Figure 3a), consistent with electrocatalytic N_2RR. Interestingly, the reversible CV response of the **Co**(III,NH)$^{2+}$/**Co**(II,NH)$^+$ couple at −1.21 V (in the absence of TsOH) is noticeably altered as (TsO)**W**$(NNH_2)^+$ is added, if scanning at a slow rate (e.g., 5-25 mV·s^{-1}); the presence of the **Co**(III,N)$^+$/**Co**(II,N) couple becomes clearly evident (Figure 3b). The implication is that as **Co**(II,NH)$^+$ is generated in the presence of (TsO)**W**$(NNH_2)^+$ a CPET step occurs that generates **Co**(III,N)$^+$, the CV response of which becomes apparent at scan rates well matched to the kinetics of this chemical step in the absence of acid.

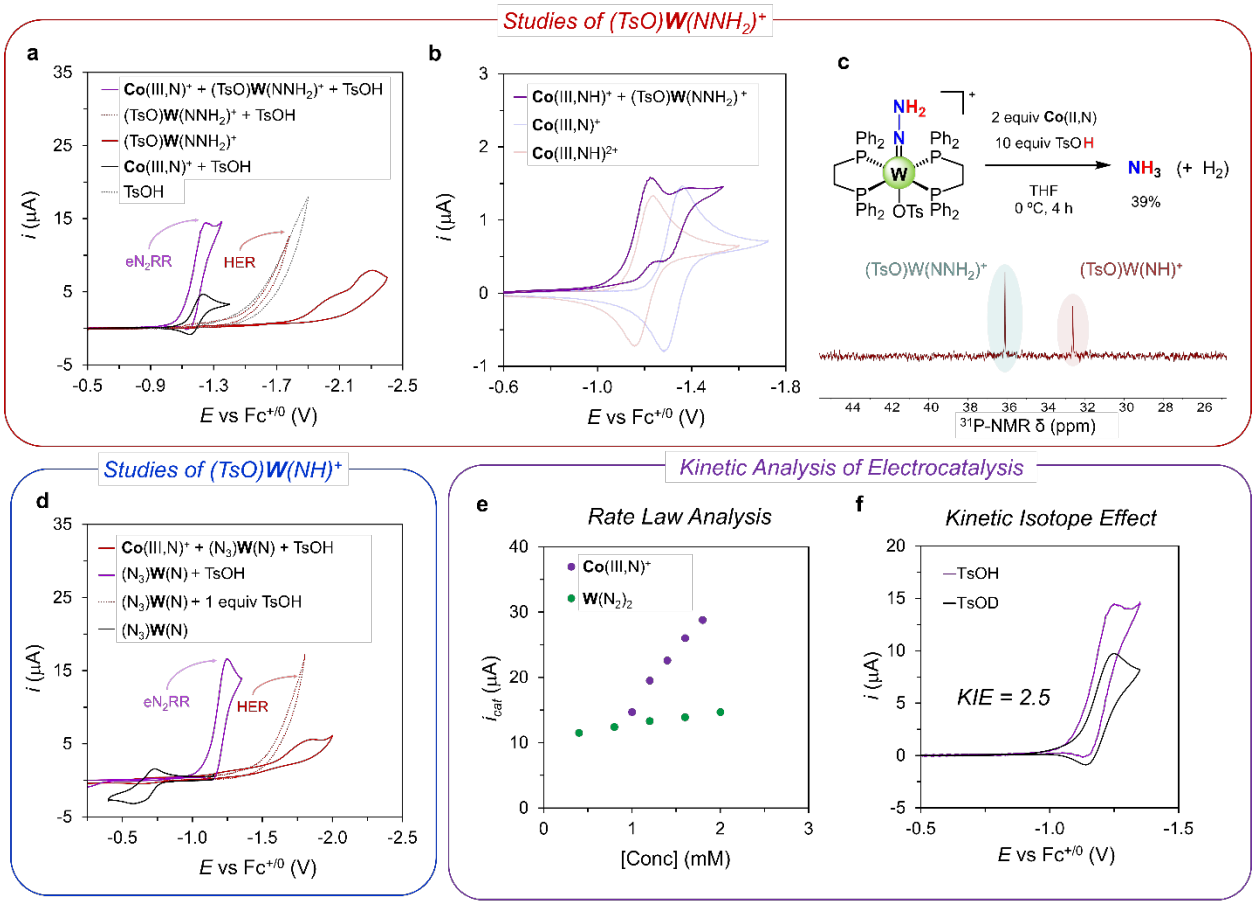

Figure 3. (a) CV of 50 mM TsOH (dashed grey); 0.5 mM **Co**(III,N)$^+$ with 50 mM TsOH (black); 0.5 mM (TsO)**W**$(NNH_2)^+$ (solid red); 50 mM TsOH and 0.5 mM (TsO)**W**$(NNH_2)^+$ (dashed red); 0.5 mM **Co**(III,N)$^+$/(TsO)**W**$(NNH_2)^+$ and 50 mM TsOH (purple). (b) CV at 5mV·s^{-1} of 0.5 mM **Co**(II,NH)$^+$/(TsO)**W**$(NNH_2)^+$ (purple trace) compared to 0.5 mM **Co**(II,NH)$^+$ (blue trace) and 0.5 mM **Co**(III,N)$^+$ (red trace). (c) Chemical reaction of 0.5 mM (TsO)**W**$(NNH_2)^+$ in THF with 2 equiv **Co**(III,N)$^+$ in THF in the presence of excess acid and the corresponding ^{31}P-NMR spectrum. (d) CV of 0.5 mM (N_3)**W**(N) (black); 0.5 mM (N_3)**W**(N) and 1 equiv TsOH (solid red); 0.5 mM (N_3)**W**(N) and 50 mM TsOH (dashed red); 0.5 mM **Co**(III,N)$^+$/(N_3)**W**(N) and

50 mM TsOH (purple). (e) Plot of the catalytic current i_{cat} versus the concentration of the different co-catalysts. (f) CV of 0.5 mM **Co**(III,N)$^+$/(TsO)**W**(NNH$_2$)$^+$ with either 50 mM TsOH (purple) or TsOD (black). **Note:** All CVs in A-F were performed at 100 mV·s^{-1} (unless otherwise stated) in 0.1 M [Li][NTf$_2$] THF solution using a BDD disk as the working electrode, Pt disk as the counter electrode and Ag/AgOTf (5mM) as the reference electrode.

To independently probe this issue, we generated (TsO)**W**(NNH$_2$)$^+$ in THF with excess TsOH present, and added two equiv of **Co**(II,N) to the solution, conditions under which **Co**(II,NH)$^+$ is instantly generated. Such a reaction liberates 0.39 equiv NH$_3$ per (TsO)**W**(NNH$_2$)$^+$ (Figure 3c) over 4 hrs (note: this experiment was performed at 0 °C to attenuate competing HER). Analysis of the reaction mixture by ^{31}P-NMR spectroscopy showed some remaining (TsO)**W**(NNH$_2$)$^+$ starting material and also a new peak corresponding to the imido complex (TsO)**W**(NH)$^+$. The identity of the latter species was confirmed by its independent generation via the protonation of the nitride precursor (N$_3$)**W**(N) with TsOH (Figure S47).[29] While other processes are presumably operative in this reaction (e.g., HER and CPET or proton-transfer (PT) steps to other W–N$_x$H$_y$ intermediates), the experiment correlates well with the CV response noted above, suggesting CPET to (TsO)**W**(NNH$_2$)$^+$ occurs, presumably followed by N–N cleavage and NH$_3$ release (Eq. 1 below depicts one plausible scenario). Such a CPET step helps explain why the system can be turned over at −1.2 V, whereas one-electron reduction of (TsO)**W**(NNH$_2$)$^+$ requires a potential of −2 V.

$$\mathbf{W}{=}\mathrm{N}{-}\mathrm{NH_2}^+ \;+\; \mathbf{Co}(\mathrm{II,NH})^+ \longrightarrow \mathbf{W}{\equiv}\mathrm{N}^+ \;+\; \mathrm{NH_3} \;+\; \mathbf{Co}(\mathrm{III,N})^+ \qquad (1)$$

Relatedly, the CV of the previously reported nitride complex (N$_3$)**W**(N) shows a reversible redox wave at −0.8 V that shifts to −1.8 V upon addition of 1 equiv of TsOH to generate (X)**W**(NH)$^+$ (X = N$_3^-$ or OTs$^-$; Figure 3d).[29–31] Including 1 equiv of **Co**(III,N)$^+$ and excess TsOH with in situ generated (TsO)**W**(NH)$^+$ yields the same multielectron electrocatalytic wave at −1.2 V observed with (TsO)**W**(NNH$_2$)$^+$. Additionally, the reaction of (N$_3$)**W**(N) with 4 equiv of **Co**(II,N) in the presence of excess TsOH afforded 0.79 equiv NH$_3$ per **W**, along with (TsO)**W**(NNH$_2$)$^+$ and (TsO)**W**(NH)$^+$ detected via ^{31}P-NMR spectroscopy (Figure S49). These experiments establish that an imide intermediate of the type (TsO)**W**(NH)$^+$ can cycle through the downstream half of the N$_2$RR cycle at −1.2 V to regenerate **W**(N$_2$)$_2$, which is then protonated to (TsO)**W**(NNH$_2$)$^+$ by the excess acid. CPET from **Co**(II,NH)$^+$ to (TsO)**W**(NH)$^+$ likely initiates this process given the 1-electron reduction potential (~ −1.8 V) for an (X)**W**(NH)$^+$ species is presumably inaccessible at our operating potential.

Kinetic analysis of the N$_2$RR electrocatalysis observed is difficult due to the 6H$^+$/6e$^-$ nature of the process, obscuring analytical solutions to the relationship between the catalytic current (i_{cat}) and the kinetic rate (k_{obs}); such an analysis is further obfuscated by the use of two co-(electro)catalysts working in tandem (see Supplementary Information, section S1). Nonetheless, by independently varying the concentration of the **W**(N$_2$)$_2$ and **Co**(III,N)$^+$, we could determine a positive order for both co-catalysts in the electrocatalytic response (Figure 3e). Interestingly, a positive order in acid was also evident (Figure S60), as was a primary kinetic isotope effect (2.5) when comparing TsOH vs TsOD (Figure 3f). These electrochemical and chemical data presented in total are consistent with one or perhaps two rate-contributing CPET steps, involving (TsO)**W**(NNH$_2$)$^+$ and possibly also (TsO)**W**(NH)$^+$, and a rate-contributing protonation step (such as initial protonation of **W**(N$_2$)$_2$; see Supplementary Information, section S6).

To explore this tandem *e*CPET-N$_2$RR strategy more broadly, we turned our attention to a series of complexes known to mediate catalytic N$_2$RR in the presence of various reductant/acid reagents (Figure 4a). We opted to test them under the standard conditions (Figure 2a; using 0.05 mM of the N$_2$RR co-catalyst in place of **W**(N$_2$)$_2$), reasoning that some degree of electrocatalysis might turn on at −1.2 V if CPET steps from **Co**(II,NH)$^+$ can circumvent the need for challenging ET steps requiring more negative potentials.

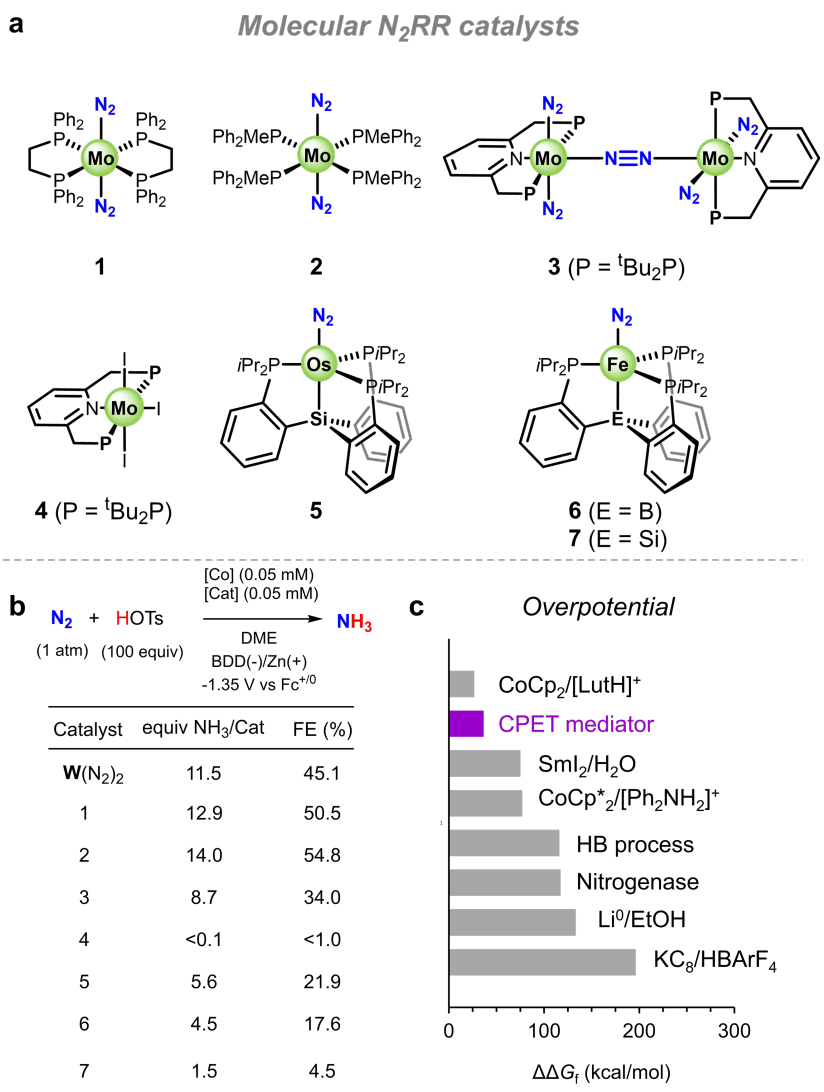

Catalyst	equiv NH_3/Cat	FE (%)
W$(N_2)_2$	11.5	45.1
1	12.9	50.5
2	14.0	54.8
3	8.7	34.0
4	<0.1	<1.0
5	5.6	21.9
6	4.5	17.6
7	1.5	4.5

Figure 4. (a) Molecular N_2RR catalysts explored in combination with the cobalt CPET mediator under electrocatalytic conditions. (b) Results of the electrocatalytic experiments for each molecular catalyst upon controlled potential electrolysis at −1.35 V vs $Fc^{+/0}$ in 0.1 M [Li][NTf_2] DME solution containing 0.05 mM **Co**(III,N)$^+$, 0.05 mM of N_2RR catalyst, and 5 mM TsOH, using a BDD plate working electrode. (c) Estimated overpotential ($\Delta\Delta G_f$) for N_2RR including the tandem *e*CPET strategy reported here, the HB process (which includes H_2 generation), a nitrogenase enzyme, Li-mediated N_2RR using EtOH as the H^+ source, and various reductant and acid partners used in chemically driven N_2RR.

To probe this, we examined the group VIII complexes **Fe**(N_2) and **Os**(N_2), where **Fe** and **Os** feature tris(phosphine)borane and silane ligands, respectively (Figure 4a). Each mediates N_2RR at -78 °C but requires a comparatively strong reductant (Cp^*_2Co at −2 V) owing to an M–$N_2^{0/-}$ couple that is key to moving through their respective N_2RR cycles via an electron transfer-proton transfer pathway (Eq. 2 and 3).[32,33] Such a pathway is not feasible at −1.2 V. Strikingly, both **Fe** and **Os** display an electrocatalytic wave at −1.2 V (see Supplementary Information, section S9), akin to **W**$(N_2)_2$, and CPE at −1.35 V produced 5.6 and 4.5 equiv NH_3, respectively (Figure 4b). Despite their relatively lower selectivity for NH_3 generation compared to **W**$(N_2)_2$, for which these conditions were optimized, the electrocatalysis observed represents a remarkable shift in thermodynamic efficiency for the overall N_2RR cycle relative to previously reported conditions using Cp^*_2Co and $Ph_2NH_2^+$ (vide infra). To explain this, we posit that the neutral M–N_2 adduct species are converted directly to M–N=NH intermediates via CPET from **Co**(II,NH)$^+$, circumventing the M–$N_2^{0/-}$ couple in the cycle (Eq. 4).[32] As a counter example, a related tris(phosphine)silyl iron-N_2 complex, (SiP_3)Fe–N_2, is electrocatalytically inactive under standard conditions, presumably due to the generation of an undesired (SiP_3)Fe(H)(N_2) state which cannot be moved through the N_2RR cycle.[12,34]

$$\mathbf{M}\text{—}N_2 + e^- \xrightarrow{< -2V} \mathbf{M}\text{—}N_2^- \qquad (2)$$

$$\mathbf{M}\text{—}N_2 + H^+ \longrightarrow \mathbf{M}\text{—}N_2H \qquad (3)$$

$$\mathbf{M}\text{—}N_2 + \mathbf{Co}(II,NH)^+ \longrightarrow \mathbf{M}\text{—}N_2H + \mathbf{Co}(III,N)^+ \qquad (4)$$

For **Fe** specifically, generation of the on-path **Fe**–N_2 species requires reduction of the **Fe**$^+$ pre-catalyst used here, which occurs at ca. −1.4 V (see Supplementary Information, section S9). Thus, applying slightly more bias in the CPE (−1.45 V instead of −1.35 V) results in improved NH_3 yield (9.3 equiv NH_3 per **Fe**). The results for **Fe** described in this study are distinct from our previous study.[17] When exploring the addition of Cp^*_2Co to **Fe** as a potential PCET mediator, a slightly enhanced yield was observed relative to when Cp^*_2Co was not added, but a potential of −2.1 V was necessary, indicating that accessing the Fe–N_2^- anion was still required.

We also explored a series of Mo complexes, including two tetrakis(phosphine) systems that are structurally related to **W**$(N_2)_2$ (compounds **1** and **2** in Figure 4a), and highly active pincer-type bis(phosphine)pyridine complexes pioneered more recently.[11,35] Among the reductants that have proven effective for these systems, SmI_2/H_2O has led to the most impressive results in chemically (as opposed to electrochemically) driven catalysis.[36,37] We find that the **Mo**$(N_2)_2$ complexes (**1**) and (**2**) are both effective co-electrocatalysts with impressive selectivities, furnishing 12.9 and 14.0 equiv NH_3 (50.5 and 54.8% FE for NH_3), respectively. A dinuclear Mo catalyst system (**3**) also displays electrocatalysis under these conditions (8.7 equiv NH_3 per Mo).[11] By contrast, the mononuclear triiodide complex (**4**), which has been demonstrated to be highly active for N_2RR,[36] is electrocatalytically inactive under these conditions (< 0.1 equiv NH_3 detected). The latter observation is readily explained; the strong reduction potential (−1.8 V) required to access an on-path N_2RR intermediate by iodide loss is not accessible at −1.35 V.[38]

The free energy for the electrocatalytic N_2RR processes described here compares quite favorably to estimates for other systems that mediate catalytic and electrocatalytic N_2RR. This can be readily quantified by $\Delta\Delta G_F(NH_3)$, a term that compares the energetic input for N_2RR relative to a reaction that derives the needed protons and electrons from H_2 (Eq. 5).[39,40] Using the bond dissociation free energy (BDFE) for H_2 (102.5 kcal/mol) [41] and that of the CPET mediator **Co**(II,NH)$^+$ (38.9 kcal/mol), [26] the $\Delta\Delta G_F(NH_3)$ is 36.5 kcal/mol for the electrocatalysis observed at −1.2 V by our CV studies. This net driving force is at least 50 kcal/mol lower than has been reported for most other reductant/acid cocktails used with synthetic N_2RR catalyst systems (Figure 4c): SmI_2/H_2O (75 kcal/mol), $Cp^*_2Co/[Ph_2NH_2]^+$ (77 kcal/mol), $KC_8/HBAr^F_4$ (196 kcal/mol) (BAr^F_4 = B(3,5-$(CF_3)_2$-$C_6H_3)_4$).[32,42] A crude comparison with the biological nitrogenases (~117 kcal/mol accounting for ATP) and the industrial HB process (~116 kcal/mol when considering *both* H_2 production and N_2 reduction) is also favorable.[43] Likewise, heterogeneous systems based on Li^+/Li ($E°(Li^{+/0})$ < −3.7 V), which are commonly partnered with ethanol as the acid, operate at an estimated $\Delta\Delta G_F(NH_3)$ = 133 kcal/mol.[7,44] Interestingly, one combination of reductant and acid, Cp_2Co and lutidinium, first studied in the Schrock system and later applied towards N_2RR catalysis with the Nishibayashi bis(phosphine)pyridine molybdenum catalyst studied herein (complex **3** in Figure 4),[10,11] is thermally favorable by comparison ($\Delta\Delta G_F(NH_3)$ = 26 kcal/mol). This suggests that alternative acids and mediator designs may yet improve the efficiency achievable by tandem electrocatalysis.

$$\Delta\Delta G_f(NH_3) = 3x[BDFE(H_2)/2 - BDFE_{eff}] \quad (5)$$

It is widely appreciated that CPET steps can offer thermodynamic advantages relative to distinct ET-PT or PT-ET pathways in enzyme catalysis, where multielectron redox reactions must be driven at biologically accessible potentials,[45] and also in synthetic catalyst systems.[9] The tandem catalytic approach to N_2RR via *e*CPET described herein provides a vivid example of the latter, where an *e*CPET step turns on catalysis that is otherwise inaccessible at the applied potential. A comparison with nitrogenase enzymes is illustrative here. It has been posited that the active-site cofactors of nitrogenases store-up proton and electron equivalents via H-atoms bound at or near to the active-site cluster to be able to mediate N_2 reduction at a single redox potential (set by the potential of the Fe-protein).[46] Our two-component tandem catalyst system functions in a conceptually similar manner, where the mediator independently stores an H-atom equivalent at a given potential for delivery to a synthetic M–N_2 "active site". While we expect this approach to small molecule reductive catalysis via *e*CPET may prove more general, exciting opportunities remain for fundamental progress and practical applications. For instance, the rate of the N_2RR electrocatalysis described here at -1.2 V, while remarkable compared to background, should be possible to enhance. In this context, fundamental studies towards developing new tandem co-catalysts, and studies aimed at improving the electrolyte, acid, and electrode interface, should prove fruitful.

SUPPLEMENTARY INFORMATION:
Supplementary Text and Data, Supplementary Table S1, and Supplementary Figures S1-S85.

Author Contributions:

P.G.B., M.J.C. and J.C.P. conceptualized the work. P.G.B. designed and executed the experiments. J.D. assisted with the execution of the catalytic experiments. All authors analyzed, interpreted the data and cowrote the manuscript.

The authors declare no competing interests.

ACKNOWLEDGMENT

We thank the Dow Next Generation Educator Funds and Instrumentation Grants for their support of the NMR facility at Caltech. We also thank the Resnick Water and Environment Laboratory at Caltech for the use of their instrumentation. We thank the following funding agencies: Department of Energy, Office of Basic Energy Sciences (DOE-0235032), Catalysis Science Program (for the development and applications of CPET mediators); National Institutes of Health (R01 GM-075757) (for studies of Fe-mediated N_2RR). P.G.B. thanks the Ramón Areces Foundation for a postdoctoral fellowship. J.D. thanks the Arnold and Mabel Beckman Foundation for a postdoctoral fellowship. M.J.C. thanks the Resnick Sustainability Institute for a graduate fellowship.

REFERENCES

(1) Erisman, J. W.; Sutton, M. A.; Galloway, J.; Klimont, Z.; Winiwarter, W. How a Century of Ammonia Synthesis Changed the World. *Nat. Geosci.* **2008**, *1* (10), 636–639.

(2) Chen, J. G.; Crooks, R. M.; Seefeldt, L. C.; Bren, K. L.; Bullock, R. M.; Darensbourg, M. Y.; Holland, P. L.; Hoffman, B.; Janik, M. J.; Jones, A. K.; Kanatzidis, M. G.; King, P.; Lancaster, K. M.; Lymar, S. V.; Pfromm, P.; Schneider, W. F.; Schrock, R. R. Beyond Fossil Fuel–Driven Nitrogen Transformations. *Science* **2018**, *360* (6391), 873–879.

(3) Service, R. F. Ammonia—a renewable fuel made from sun, air, and water—could power the globe without carbon https://www.sciencemag.org/news/2018/07/ammonia-renewable-fuel-made-sun-air-and-water-could-power-globe-without-carbon (accessed 2021-08-20).

(4) Martín, A. J.; Shinagawa, T.; Pérez-Ramírez, J. Electrocatalytic Reduction of Nitrogen: From Haber-Bosch to Ammonia Artificial Leaf. *Chem* **2019**, *5* (2), 263–283.

(5) Qing, G.; Ghazfar, R.; Jackowski, S. T.; Habibzadeh, F.; Ashtiani, M. M.; Chen, C.-P.; Smith, M. R.; Hamann, T. W. Recent Advances and Challenges of Electrocatalytic N_2 Reduction to Ammonia. *Chem. Rev.* **2020**, *120* (12), 5437–5516.

(6) Deng, J.; Iñiguez, J. A.; Liu, C. Electrocatalytic Nitrogen Reduction at Low Temperature. *Joule* **2018**, *2* (5), 846–856.

(7) Lazouski, N.; Schiffer, Z. J.; Williams, K.; Manthiram, K. Understanding Continuous Lithium-Mediated Electrochemical Nitrogen Reduction. *Joule* **2019**, *3* (4), 1127–1139.

(8) Ren, Y.; Yu, C.; Tan, X.; Huang, H.; Wei, Q.; Qiu, J. Strategies to Suppress Hydrogen Evolution for Highly Selective Electrocatalytic Nitrogen Reduction: Challenges and Perspectives. *Energy Environ. Sci.* **2021**, *14* (3), 1176–1193.

(9) Chalkley, M. J.; Drover, M. W.; Peters, J. C. Catalytic N_2-to-NH_3 (or -N_2H_4) Conversion by Well-Defined Molecular Coordination Complexes. *Chem. Rev.* **2020**, *120* (12), 5582–5636.

(10) Yandulov, D. V.; Schrock, R. R. Catalytic Reduction of Dinitrogen to Ammonia at a Single Molybdenum Center. *Science* **2003**, *301* (5629), 76–78.

(11) Arashiba, K.; Miyake, Y.; Nishibayashi, Y. A Molybdenum Complex Bearing PNP-Type Pincer Ligands Leads to the Catalytic Reduction of Dinitrogen into Ammonia. *Nat. Chem.* **2010**, *3*, 120–125.

(12) Anderson, J. S.; Rittle, J.; Peters, J. C. Catalytic Conversion of Nitrogen to Ammonia by an Iron Model Complex. *Nature* **2013**, *501* (7465), 84–87.

(13) Lee, Y. S.; Ruff, A.; Cai, R.; Lim, K.; Schuhmann, W.; Minteer, S. D. Electroenzymatic Nitrogen Fixation Using a MoFe Protein System Immobilized in an Organic Redox Polymer. *Ang. Chem. Int. Ed.* **2020**, *59* (38), 16511–16516.

(14) Lindley, B. M.; van Alten, R. S.; Finger, M.; Schendzielorz, F.; Würtele, C.; Miller, A. J. M.; Siewert, I.; Schneider, S. Mechanism of Chemical and Electrochemical N_2 Splitting by a Rhenium Pincer Complex. *J. Am. Chem. Soc.* **2018**, *140* (25), 7922–7935.

(15) Merakeb, L.; Robert, M. Advances in Molecular Electrochemical Activation of Dinitrogen. *Current Opinion in Electrochemistry* **2021**, *29*, 100834.

(16) Bruch, Q. J.; Connor, G. P.; McMillion, N. D.; Goldman, A. S.; Hasanayn, F.; Holland, P. L.; Miller, A. J. M. Considering Electrocatalytic Ammonia Synthesis via Bimetallic Dinitrogen Cleavage. *ACS Catal.* **2020**, *10* (19), 10826–10846.

(17) Chalkley, M. J.; Del Castillo, T. J.; Matson, B. D.; Peters, J. C. Fe-Mediated Nitrogen Fixation with a Metallocene Mediator: Exploring PKa Effects and Demonstrating Electrocatalysis. *J. Am. Chem. Soc.* **2018**, *140* (19), 6122–6129.

(18) Helm, M. L.; Stewart, M. P.; Bullock, R. M.; DuBois, M. R.; DuBois, D. L. A Synthetic Nickel Electrocatalyst with a Turnover Frequency Above 100,000 S−1 for H2 Production. *Science* **2011**, *333* (6044), 863–866.

(19) Francke, R.; Schille, B.; Roemelt, M. Homogeneously Catalyzed Electroreduction of Carbon Dioxide—Methods, Mechanisms, and Catalysts. *Chem. Rev.* **2018**, *118* (9), 4631–4701.

(20) Pegis, M. L.; Wise, C. F.; Martin, D. J.; Mayer, J. M. Oxygen Reduction by Homogeneous Molecular Catalysts and Electrocatalysts. *Chem. Rev.* **2018**, *118* (5), 2340–2391.

(21) Benson, E. E.; Kubiak, C. P.; Sathrum, A. J.; Smieja, J. M. Electrocatalytic and Homogeneous Approaches to Conversion of CO_2 to Liquid Fuels. *Chem. Soc. Rev.* **2008**, *38* (1), 89–99.

(22) Pickett, C. J.; Talarmin, J. Electrosynthesis of Ammonia. *Nature* **1985**, *317* (6038), 652–653.

(23) Becker, J. Y.; Avraham (Tsarfaty), S. Nitrogen Fixation: Part III. Electrochemical Reduction of Hydrazido (-NNH_2) Mo and W Complexes. Selective Formation of NH_3 under Mild Conditions. *J. Electroanal. Chem. Interf. Electrochem.* **1990**, *280* (1), 119–127.

(24) Wang, Y.; Montoya, J. H.; Tsai, C.; Ahlquist, M. S. G.; Nørskov, J. K.; Studt, F. Scaling Relationships for Binding Energies of Transition Metal Complexes. *Catal. Lett.* **2016**, *146* (2), 304–308.

(25) Kuriyama, S.; Arashiba, K.; Nakajima, K.; Tanaka, H.; Kamaru, N.; Yoshizawa, K.; Nishibayashi, Y. Catalytic Formation of Ammonia from Molecular Dinitrogen by Use of Dinitrogen-Bridged Dimolybdenum–Dinitrogen Complexes Bearing PNP-Pincer Ligands: Remarkable Effect of Substituent at PNP-Pincer Ligand. *J. Am. Chem. Soc.* **2014**, *136* (27), 9719–9731.

(26) Chalkley, M. J.; Garrido-Barros, P.; Peters, J. C. A Molecular Mediator for Reductive Concerted Proton-Electron Transfers via Electrocatalysis. *Science* **2020**, *369* (6505), 850–854.

(27) Derosa, J.; Garrido-Barros, P.; Peters, J. C. Electrocatalytic Reduction of C–C π-Bonds via a Cobaltocene-Derived Concerted Proton–Electron Transfer Mediator: Fumarate Hydrogenation as a Model Study. *J. Am. Chem. Soc.* **2021**, *143* (25), 9303–9307.

(28) Martin, H. B.; Argoitia, A.; Landau, U.; Anderson, A. B.; Angus, J. C. Hydrogen and Oxygen Evolution on Boron-Doped Diamond Electrodes. *J. Electrochem. Soc.* **1996**, *143* (6), L133–L136.

(29) Bevan, P. C.; Chatt, J.; Dilworth, J. R.; Henderson, R. A.; Leigh, G. J. The Preparation and Reactions of Azidobis[1,2-Bis(Diphenylphosphino)-Ethane]Nitridotungsten(IV). *J. Chem. Soc., Dalton Trans.* **1982**, No. 4, 821–824.

(30) Mohammed, M. Y.; Pickett, C. J. From Metal Imides and Molecular Nitrogen to Ammonia and Dinitrogen Complexes. *J. Chem. Soc., Chem. Commun.* **1988**, No. 16, 1119–1121.

(31) Alias, Y.; Ibrahim, S. K.; Queiros, M. A.; Fonseca, A.; Talarmin, J.; Volant, F.; Pickett, C. J. Electrochemistry of Molybdenum Imides: Cleavage of Molybdenum–Nitrogen Triple Bonds to Release Ammonia or Amines†. *J. Chem. Soc., Dalton Trans.* **1997**, No. 24, 4807–4816.

(32) Chalkley, M. J.; Del Castillo, T. J.; Matson, B. D.; Roddy, J. P.; Peters, J. C. Catalytic N_2-to-NH_3 Conversion by Fe at Lower Driving Force: A Proposed Role for Metallocene-Mediated PCET. *ACS Cent. Sci.* **2017**, *3* (3), 217–223.

(33) Fajardo Jr., J.; Peters, J. C. Catalytic Nitrogen-to-Ammonia Conversion by Osmium and Ruthenium Complexes. *J. Am. Chem. Soc.* **2017**, *139* (45), 16105–16108.

(34) Fong, H.; Moret, M.-E.; Lee, Y.; Peters, J. C. Heterolytic H_2 Cleavage and Catalytic Hydrogenation by an Iron Metallaboratrane. *Organometallics* **2013**, *32* (10), 3053–3062.

(35) Chatt, J.; Leigh, G. J. Nitrogen Fixation. *Chem. Soc. Rev.* **1972**, *1* (1), 121–144.

(36) Ashida, Y.; Arashiba, K.; Nakajima, K.; Nishibayashi, Y. Molybdenum-Catalysed Ammonia Production with Samarium Diiodide and Alcohols or Water. *Nature* **2019**, *568* (7753), 536–540.

(37) Ashida, Y.; Arashiba, K.; Tanaka, H.; Egi, A.; Nakajima, K.; Yoshizawa, K.; Nishibayashi, Y. Molybdenum-Catalyzed Ammonia Formation Using Simple Monodentate and Bidentate Phosphines as Auxiliary Ligands. *Inorg. Chem.* **2019**, *58* (14), 8927–8932.

(38) Arashiba, K.; Eizawa, A.; Tanaka, H.; Nakajima, K.; Yoshizawa, K.; Nishibayashi, Y. Catalytic Nitrogen Fixation via Direct Cleavage of Nitrogen–Nitrogen Triple Bond of Molecular Dinitrogen under Ambient Reaction Conditions. *Bull. Chem. Soc. Jpn.* **2017**, *90* (10), 1111–1118.

(39) Chalkley, M. J.; Peters, J. C. Relating N–H Bond Strengths to the Overpotential for Catalytic Nitrogen Fixation. *Eur. J. Inorg. Chem.* **2020**, *2020* (15–16), 1353–1357.

(40) Pappas, I.; Chirik, P. J. Catalytic Proton Coupled Electron Transfer from Metal Hydrides to Titanocene Amides, Hydrazides and Imides: Determination of Thermodynamic Parameters Relevant to Nitrogen Fixation. *J. Am. Chem. Soc.* **2016**, *138* (40), 13379–13389.

(41) Warren, J. J., Tronic, T. A. & Mayer, J. M. Thermochemistry of Proton-Coupled Electron Transfer Reagents and its Implications *Chem. Rev.* **2010**, *110*, 6961–7001.

(42) Kolmar, S. S.; Mayer, J. M. $SmI_2(H_2O)_n$ Reduction of Electron Rich Enamines by Proton-Coupled Electron Transfer. *J. Am. Chem. Soc.* **2017**, *139* (31), 10687–10692.

(43) van der Ham, C. J. M.; Koper, M. T. M.; Hetterscheid, D. G. H. Challenges in Reduction of Dinitrogen by Proton and Electron Transfer. *Chem. Soc. Rev.* **2014**, *43* (15), 5183–5191.

(44) Lazouski, N.; Chung, M.; Williams, K.; Gala, M. L.; Manthiram, K. Non-Aqueous Gas Diffusion Electrodes for Rapid Ammonia Synthesis from Nitrogen and Water-Splitting-Derived Hydrogen. *Nat. Catal.* **2020**, *3* (5), 463–469.

(45) Reece, S. Y.; Nocera, D. G. Proton-Coupled Electron Transfer in Biology: Results from Synergistic Studies in Natural and Model Systems. *Annu. Rev. Biochem.* **2009**, *78* (1), 673–699.

(46) Lanzilotta, W. N.; Christiansen, J.; Dean, D. R.; Seefeldt, L. C. Evidence for Coupled Electron and Proton Transfer in the [8Fe-7S] Cluster of Nitrogenase. *Biochemistry* **1998**, *37* (32), 11376–11384.